NMe_2 and OCH_2CH_3), 4.5-5.3 (m, 3, 3CH), 6.34 (s, 1, CHOEt), 8.40 and 9.38 (both s, 2, 2 purine CH). *Anal.* ($C_{17}H_{24}N_6O_3$) C, H, N.

The yellow glass **9a** was dissolved in 2 *N* HCl (50 ml) and the solution stirred for 10 min. The pH was then adjusted to 9 by addition of 6 *N* NaOH (*ca.* 23 ml). The resulting solution was saturated with NaCl and then extracted with $CHCl_3$ (3 × 100 ml). The $CHCl_3$ solution was dried ($CaSO_4$) and then evaporated, leaving **10a** as a white solid foam (4.27 g, 70% from **7a**), sufficiently pure for use. Chromatography on a preparative tlc plate developed in 10% MeOH-$CHCl_3$ gave a sample which crystallized with difficulty from EtOAc: mp 85–88°; $[\alpha]_{589}$ −18.0°, $[\alpha]_{578}$ −18.9°, $[\alpha]_{546}$ −21.8°, $[\alpha]_{436}$ −40.4°, $[\alpha]_{365}$ −78.8° (*c* 1.3, MeOH); ir similar to that of racemate **10**, identical with that of enantiomer **10b**. *Anal.* ($C_{14}H_{20}N_6O_2$) C, H, N.

A sample of the enantiomer **10b** was prepared in the same way from **9b**. An analytical sample was prepared by chromatography, giving **10b** as a white crystals: mp 85–88°; $[\alpha]_{589}$ +17.9°, $[\alpha]_{578}$ +18.9°, $[\alpha]_{546}$ +21.8°, $[\alpha]_{436}$ +40.4°, $[\alpha]_{365}$ +78.8° (*c* 1.0, MeOH). *Anal.* C, H, N.

A sample of the racemate **10** was prepared in the same way from **9**. Crystallization from EtOAc gave **10** as white granules (72% from **7**): mp 147–150°. Recrystallization from EtOAc gave white granules: mp 150–151°; mixture melting point with an authentic sample prepared by an alternate route[2] undepressed; and ir identical with that of the authentic sample.

References

(1) R. G. Almquist and R. Vince, *J. Med. Chem.*, **16**, 1396 (1973) (previous paper).
(2) S. Daluge and R. Vince, *J. Med. Chem.*, **15**, 171 (1972).
(3) R. Vince, S. Daluge, and M. Palm, *Biochem. Biophys. Res. Commun.*, **46**, 866 (1972).
(4) S. Pestka, R. Vince, S. Daluge, and R. Harris, *Antimicrob. Ag. Chemother.*, 4, 37 (1973).
(5) M. Furdík and E. Sidóová, *Acta Fac. Rerum Natur. Univ. Comenianae, Chim.*, **9**, 269 (1965); *Chem. Abstr.*, **63**, 13095*a* (1965).
(6) Y. Kawai, *Nippon Kagaku Zasshi*, **81**, 1606 (1960); *Chem. Abstr.*, **56**, 2341*b* (1962).
(7) R. B. Moffett in "Organic Syntheses," Collect. Vol. IV, N. Rabjohn, Ed., Wiley, New York, N. Y., 1963, p 238.
(8) (a) K. Kochloefl, V. Bažant, and F. Šorm, *Chem. Listy*, **49**, 519 (1955); (b) L. F. Hatch and G. Bachmann, *Chem. Ber.*, **97**, 132 (1964).
(9) L. Goodman, S. Winstein, and R. Boschan, *J. Amer. Chem. Soc.*, **80**, 4312 (1958).
(10) (a) E. L. Eliel, "Stereochemistry of Carbon Compounds," McGraw-Hill, New York, N. Y., 1962, p 294, and references cited therein; (b) A. Hasegawa and H. Z. Sable, *J. Org. Chem.*, **31**, 4154 (1966).
(11) R. E. Parker and N. S. Isaac, *Chem. Rev.*, **59**, 737 (1959).
(12) H. J. Schaeffer and C. F. Schwender in "Synthetic Procedures in Nucleic Acid Chemistry," Vol. 1, W. W. Zorbach and R. S. Tipson, Ed., Interscience, New York, N. Y., 1968, pp 6–7.
(13) N. Yathindra and M. Sundaralingam, *Biochim. Biophys. Acta*, **308**, 17 (1973).
(14) D. Nathans and A. Neidle, *Nature (London)*, **197**, 1076 (1963).
(15) R. H. Symons, R. J. Harris, L. P. Clarke, J. F. Wheldrake, and W. H. Elliott, *Biochim. Biophys. Acta*, **179**, 248 (1969).
(16) R. J. Harris and R. H. Symons, *Bioorg. Chem.*, **2**, 286 (1973).
(17) I. Rychlík, J. Černá, S. Chládek, P. Pulkrábek, and J. Žemlička, *Eur. J. Biochem.*, **16**, 136 (1970).
(18) C. Coutsogeorgopoulos, *Biochim. Biophys. Acta*, **129**, 214 (1966).
(19) R. J. Harris, J. E. Hanlon, and R. H. Symons, *Biochim. Biophys. Acta*, **240**, 244 (1971).

Ab Initio Calculations on Large Molecules Using Molecular Fragments. Lincomycin Model Studies†

Lester L. Shipman,‡ Ralph E. Christoffersen,*,§

Department of Chemistry, University of Kansas, Lawrence, Kansas 66044

and B. Vernon Cheney

Research Laboratories of The Upjohn Company, Kalamazoo, Michigan 49001.

Received October 29, 1973

Ab initio Hartree-Fock SCF calculations have been carried out using the molecular fragment approach for a series of molecular species, chosen to model the pyrrolidine and amide portions of the antibiotic lincomycin as well as portions of the carbohydrate moiety in several analogs. The effects of various chemical modifications on the electronic structure and preferred conformations are studied and related to available experimental data. It is found that protonation of the nitrogen atom of the pyrrolidine ring modifies the electronic structure of the ring substantially, and the likely effect of protonation on antibacterial activity is discussed. In addition, modifications of the sugar side chain can cause interactions with the amide and pyrrolidine moieties, and the effect of these interactions on conformational stability and antibacterial activity is discussed.

Lincomycin (see Figure 1) is an antibiotic produced by *Streptomyces lincolnensis* which has been shown to be effective against gram-positive bacteria.[1-4] Currently available evidence indicates that lincomycin inhibits protein synthesis by acting at the 50S ribosomal subunit.[5-13] However, the precise mode of action has not been clearly established by the studies conducted thus far. A theoretical model which rationalizes many structure-activity relationships of lincomycin-related antibiotics is presented in the companion paper.[14]

Chemical modification of the lincomycin molecule has produced a series of analogs with significantly different potency than lincomycin.[15] Among the most interesting analogs are those differing only in the nature and/or configuration of the C(7) substituents. For example, lincomycin, which possesses an *R* configuration at C(7), is twice as effective in the standard plate assay with *Sarcina lutea* as the *S* stereoisomer, 7-epilincomycin. Furthermore, 7(*S*)-chloro-7-deoxylincomycin (clindamycin) and 7(*R*)-chloro-7-deoxylincomycin (7-epiclindamycin) are both more effective than lincomycin in the *S. lutea* assay; the activity of clindamycin shows a fourfold enhancement while 7-epiclindamycin exhibits a twofold improvement. As yet, no satisfactory rationale for these differences has been suggested.

†This study was supported in part by the University of Kansas and by grants from the National Science Foundation and The Upjohn Co., Kalamazoo, Mich. 49001.

‡NSF Trainee, 1969-1972.
§Alfred P. Sloan Research Fellow, 1971-1973. Author to whom requests for reprints should be addressed.

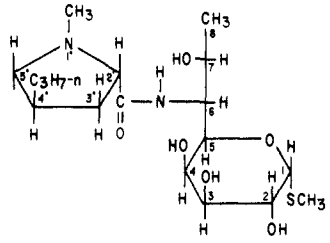

Figure 1. Lincomycin.

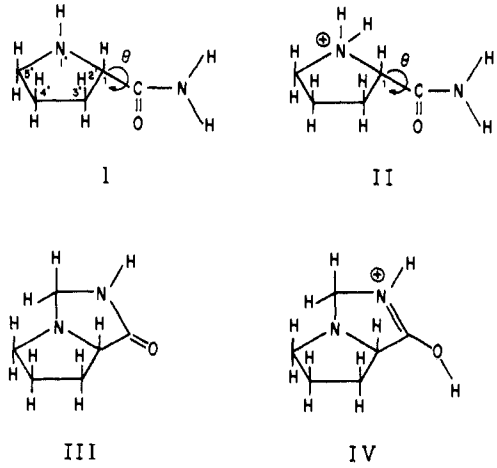

Figure 2. Models of 2-pyrrolidinecarboxylamide moiety.

In the current study, L-prolinamide has been used to characterize the pyrrolidine and attached amide unit portions of the lincomycin molecule. Additional calculations have been performed on *N*-(1-hydroxy-3-R-2-butyl)acetamide, where R = OH or Cl, in order to simulate the environment of the sugar side chain in lincomycin, 7-epilincomycin, clindamycin, and 7-epiclindamycin. The effects of chemical modification on the electronic structure and molecular conformation have been studied *via ab initio* molecular fragment SCF calculations,[16-30] in order to quantify the kinds of interactions to be expected in these moieties. The molecular fragment basis sets used in these calculations are completely specified in Table I.

Several molecular species, I-IV, that were considered as models of the pyrrolidine and attached amide unit portions of lincomycin in the current study are shown in Figure 2. The nuclear geometry of the pyrrolidine ring in I-IV and the amide unit in I and II were essentially taken from the X-ray geometry of lincomycin hydrochloride.[31] The amide unit geometry in III and IV was estimated from the X-ray geometry of cycloserine.[32] The molecular species, V-XII, employed to investigate the effects of chloro and hydroxyl substituents at position 7 in the sugar moiety of lincomycin are shown in Figure 3. Geometries for the chlorine-containing molecules were taken from the X-ray data of clindamycin hydrochloride monohydrate. In order to provide a point of reference to the lincomycin molecule and to facilitate discussion, the atoms in the model structures portrayed in Figures 2 and 3 have been arbitrarily numbered in accordance with the convention which has been adopted for lincomycin.

Conformational Energies. The total energies of species I and II (see Figure 2) were followed as a function of θ. θ [$\angle$C(3′)-C(2′)-C(A)-O(A) for I, where C(A) and O(A) designate the carbonyl atoms of the amide unit] is the dihedral angle that specifies the conformational relationship between the pyrrolidine ring and the amide unit. In I, θ = 0° is the angle at which the C(A)-O(A) and C(2′)-C(3′) bonds are eclipsed, $\theta \approx 120°$ is the angle at which the C(A)-O(A) and C(2′)-N(1′) bonds are eclipsed, and $\theta \approx 240°$ is the angle at which the C(A)-O(A) and C(2′)-H(2′) bonds are eclipsed. θ is defined analogously for species II-IV and IX-XII. θ is restricted to only $\theta \approx 300°$ in species III and IV because of the constraint of ring formation.

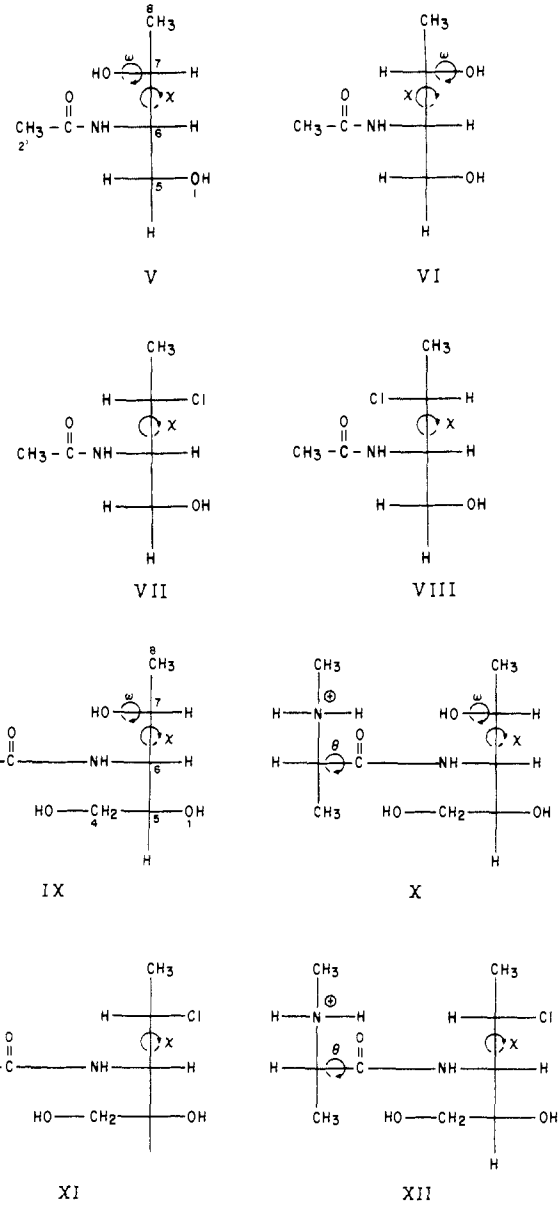

Figure 3. Models of substituted *N*-methylacetamide moiety.

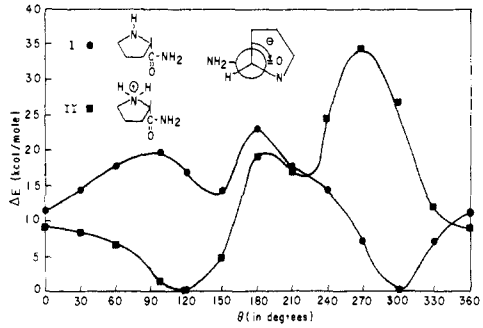

Figure 4. Conformational energy *vs.* θ curves for species I and II. Each curve has been independently zeroed at the lowest calculated energy conformation.

[=] D. J. Duchamp, The Upjohn Co., private communication.

Table I. Molecular Fragment Data[a]

Fragment type	FSGO type	FSGO distance from "heavy" atom	FSGO radii	Species in which fragment was used
CH_4 (T_d), R(C,H) = 2.05982176	C–H	1.23379402	1.67251562	I–XII
	C inner shell	0.0	0.32784375	
$\cdot CH_3$ (sp^2), R(C,H) = 1.78562447	C–H	1.13093139	1.51399487	I–XII
	C–π	±0.1	1.80394801	
	C inner shell	0.0	0.32682735	
NH_4^+ (T_d), R(N,H) = 1.95021656	N–H	0.80547793	1.50046875	II, X, XII
	N inner shell	0.0	0.27770068	
$:NH_3$ (sp^3), R(N,H) = 1.93131912	N–H	0.88573239	1.53557305	I
	N–LP	0.25630919	1.58812372	
	N inner shell	0.00101043[b]	0.27735920	
$:NH_3$ (sp^3), R(N,H) = 1.91242167	N–H	0.87735349	1.52791683	III, IV, IX, XI
	N–LP	0.25523498	1.58328000	
	N inner shell	0.00099090[b]	0.27732014	
$:NH_3$ (sp^2), R(N,H) = 1.93131910	N–H	0.75201903	1.39424495	I–XII
	N–π	±0.1	1.50625972	
	N inner shell	0.0	0.27684894	
NH_3^+ (sp^2), R(N,H) = 1.87084729	N–H	1.43289062	1.43289062	IV
	N–π	±0.1	1.27477905	
	N inner shell	0.0	0.27768390	
H_2O (sp^2), R(O,H) = 1.81415494	O–H	0.89817053	1.37154785	IV
	O–LP	0.43956045	1.30597656	
	O–π	±0.1	1.12771117	
	O inner shell	0.00105807[c]	0.24112528	
$\cdot OH$ (sp^2), R(O,H) = 1.81415494	O–H	0.72000000	1.33207031	I, II
	O–LP	0.21978022	1.31823242	
	O–π	±0.21978022	1.05151794	
	O inner shell	0.00056894[d]	0.24023926	
$\cdot OH$ (sp), R(O,H) = 1.54774058	O–H	0.76467773	1.23671871	III, V–XII
	O–LP (σ)	0.21614258	1.28753780	
	O–LP (p)	±0.1	1.19741696	
	O–π	±0.1	1.12242182	
	O inner shell	0.00057129[d]	0.24028227	
H_2O (sp^3),[e] R(O,H) = 1.81415494	O–H	0.74365356	1.35682617	V–XII
	O–LP	0.43956044	1.30568359	
	O inner shell	0.00077105[f]	0.24051208	
HCl (sp^3),[g] R(Cl,H) = 2.40754389	Cl–H	1.42011414	1.57674255	VII, VIII, XI, XII
	Cl–LP	0.98360656	1.61593323	
	Cl L shell	0.15564202	0.42207336	
	Cl K shell	0.00001750	0.10780945	

[a]All distances are reported in atomic units (1 au = 0.529172 Å). See H. Shull and G. G. Hall, *Nature* (*London*), **184,** 1559 (1959). [b]This is the distance from the nitrogen nucleus along the C_3 axis away from the lone pair. [c]This is the distance from the oxygen nucleus along the C_2 axis away from the σ lone pair. [d]This is the distance from the oxygen nucleus along the OH bond toward the hydrogen nucleus. [e]Polarization of the lone-pair orbitals causes deviations from sp^3 hybridization. The angle, ∠LOL (in degrees), formed by lines from the centers of the lone-pair orbitals to the oxygen nucleus is adjusted to account for the polarization by means of the following relationship: ∠LOL = 215.5629 − 1.083117∠HPH − 0.003312919-∠HOH[2]. [f]Distance measured along the C_2 axis from the O nucleus toward the region where the hydrogen atoms are located. [g]The arrangement of orbitals in the HCl fragment is shown schematically in the following diagram.

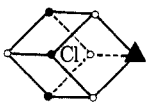

The chlorine nucleus is positioned at the center of the cube and the orbitals associated with the fragment are located on lines directed from the center through the corners of the box. The symbol ▲ fixes the line upon which the H nucleus, bond orbital, and K-shell FSGO are positioned. The corners marked with ○ and ● fix the lines for the L-shell and lone-pair orbitals, respectively.

The conformational energy *vs.* θ curves for species I and II are displayed in Figure 4, and each conformational energy curve has been independently zeroed at the lowest calculated energy conformation. Energies were calculated at 30° increments in θ for species I and II, except that the point θ = 90° was replaced by the point θ = 97.29°, which corresponds to the angle found in an X-ray crystallographic study.[31]

The absolute minimum for I occurs at $\theta \approx 300°$. In this conformation, a hydrogen bond is formed between the amide hydrogen corresponding to that of lincomycin and the pyrrolidine nitrogen [N(1′)], forming an approximately planar five-membered ring structure. On the other hand, the conformational energy curve for II (the protonated form of I) has an absolute minimum at $\theta \approx 120°$. In this conformation, a different hydrogen bond is formed between the amide oxygen [O(A)] and the quaternary amine hydrogen cis to the amide unit from pyrrolidine, forming another approximately planar five-membered ring structure. It should be emphasized that the conformational energy curves for I and II are quite different, implying that in solution the populations of the various conformers are dependent on pH. The species (similar to I) in which the pyrrolidine N–H is cis to the amide unit have not been considered, since, in lincomycin, this group is a methyl group instead of a hydrogen, and the methyl group

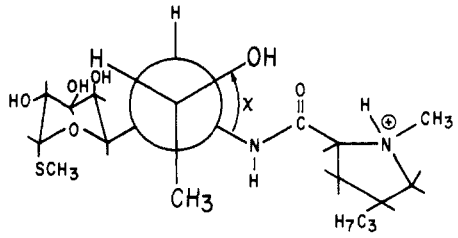

Figure 5. Newman projection of the lincomycin molecule viewed along bond from C(7) and C(6).

would be expected to be trans to the amide group for steric reasons.

Thus, a consideration of the conformational energy curves for I and II leads to the conclusion that the absolute minimum energy conformation for unprotonated (at pyrrolidine N) lincomycin as a function of θ is expected to be near $\theta = 300°$, and the absolute minimum for protonated (at pyrrolidine N) lincomycin is expected to be near $\theta = 120°$. The stability of this "protonated conformation" is supported by the results of an X-ray crystallographic study of lincomycin hydrochloride by Davis and Parthasarathy,[31] in which the value of θ was found to be 97.29. In the current study, the energy of the $\theta = 97.29°$ conformation was found to be only 1.2 kcal/mol above the energy of the absolute minimum at $\theta \approx 120°$.

The large difference in preferred conformation between protonated and unprotonated lincomycin takes on added significance in light of the conclusion by Heman-Ackah and Garrett[12] that the unprotonated form of lincomycin is responsible for its antibacterial activity. Also, it has been found that, when formaldehyde is condensed with lincomycin or an active analog to form an imidazolidine ring (similar to III) utilizing the pyrrolidine and amide nitrogens, the resulting product is biologically active *in vitro* and *in vivo*.** Ring formation, of course, fixes the pyrrolidine and amide units in the conformation at $\theta \approx 300°$, which has been predicted to be the most stable conformation for unprotonated lincomycin in the current study. Thus, it appears that there may be an optimum conformation for lincomycin for biological activity, occurring at $\theta \approx 300°$.

A Newman projection of the lincomycin X-ray structure viewed along the bond from C(7) to C(6) is presented in Figure 5. It is noted that rotation about the C(6)-C(7) bond brings the 7-OH and 8-CH_3 groups into proximity with the amide unit as well as C(5), H(5), and O(1) of the pyranose ring. However, other portions of the molecule, more distantly removed from the C(6)-C(7) bond, may have a less important effect on the rotational motion. For this reason, species V is utilized as a simple model which incorporates the major interactions that occur in the lincomycin molecule upon rotation about the C(6)-C(7) bond. In a similar manner, structures VI-VIII simulate the major interactions in 7-epilincomycin, clindamycin, and 7-epiclindamycin, respectively. Although these model structures would not be adequate to investigate rotation about the C(5)-C(6) and C(6)-N(A) bonds in the sugar side chain, it is assumed that steric constraints favor the conformation observed in the X-ray structures of lincomycin and clindamycin.†† Evidence supporting this assumption is provided by nmr data[33] which show that the conformation about the C(5)-C(6) bond is the same in aqueous solution as in the solid state for these molecules.

In using models V-VIII to investigate the preferred conformation about the C(6)-C(7) bond, only values of χ [$\angle$N(A)-C(6)-C(7)-X, where X = O(7), Cl(7)] which yield a staggered configuration were employed in the calculations since serious steric conflicts occur when the bulky groups attached to C(6) and C(7) tend to eclipse one another. Owing to the possibility of forming intramolecular hydrogen bonds involving the 7-OH group, rotation about the C(7)-O(7) bond was also considered in species V and VI. In these cases, ω [$\angle$C(6)-C(7)-O(7)-HO(7)] was varied in 60° increments from 0 to 300°.

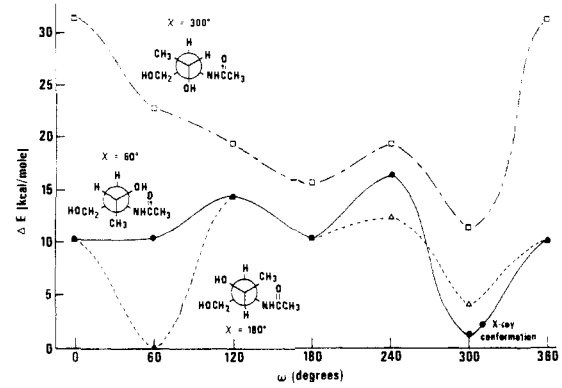

Figure 6. Conformational energy as a function of ω for various values of χ in the lincomycin moiety, V.

The conformational energy curves for V are portrayed in Figure 6. As a result of severe repulsions between 8-CH_3 and O(1), the conformation with $\chi \approx 300°$ is the least favored regardless of the value of ω. The lowest energy conformation is found when $\chi \approx 180°$ and $\omega \approx 60°$. In this case, there is an intramolecular hydrogen bond between HO(7) and O(1) which serves to stabilize the conformation. A secondary minimum occurs at $\chi \approx 60°$ and $\omega \approx 300°$, which is very close to the geometry of the lincomycin X-ray structure. Although there is an energy separation of 1.4 kcal/mol between the primary and secondary minima, the difference may not be significant due to the frequent overestimation of rotation barriers in the molecular fragment procedure.‡‡ In any case, the energies of the two states are similar enough that interactions not included in the simple model (*e.g.*, long-range intra- and intermolecular forces) may be decisive in determining the favored conformation about the C(6)-C(7) bond in lincomycin. For example, a hydrogen-bonding solvent, such as water, would likely disrupt the intramolecular hydrogen bond in order to produce two (or more) hydrogen bonds through solvent-solute interactions. Thus, the pmr spectrum of lincomycin indicates that the conformation with $\chi = 60°$ is favored in D_2O solution.[33]

As shown in Figure 7, the conformation of VI yielding the lowest energy is found at $\chi = 180°$ and $\omega = 60°$. Since all other conformations exhibit calculated energies exceeding 5 kcal/mol above the minimum, the effects of long-range interactions are less likely to stabilize the molecule in a different conformation. Hydrogen bonding between HO(7) and O(1) apparently provides the major contribution to the stability of the favored conformation in species VI as well as V.

Tables II and III contain the results of calculations util-

**A. D. Argoudelis, The Upjohn Co., private communication.

††X-Ray studies (ref 31) indicate that the hydrogens on C(5) and C(6) are trans. The hydrogens on C(6) and N(A) are also trans.

‡‡This exaggeration of barriers that is observed is generally a constant amount for rotation around similar kinds of bonds (*e.g.*, C-C bonds), although the particular amount varies for different bonds. This has the result that conformational energy surfaces predicted by the molecular fragment technique are too restrictive and may not show the proper amount of molecular flexibility. See ref 34 for a more complete discussion of the advantages and disadvantages of the initial formulation of the molecular fragment method as used here.

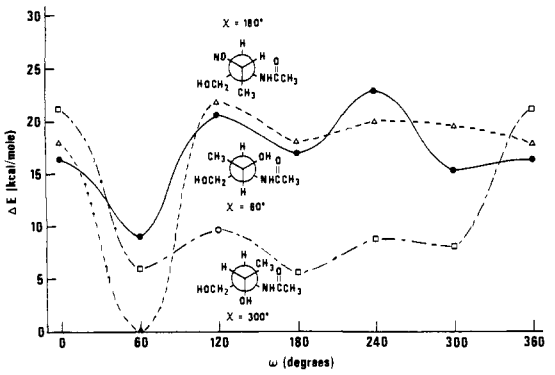

Figure 7. Conformational energy as a function of ω for various values of χ in the 7-epilincomycin moiety, VI.

izing the 7-chloro-7-deoxy models, VII and VIII. Species VII exhibits a highly stable conformation when χ = 300°, which corresponds with nmr findings[33] and the X-ray structure of clindamycin. The lowest energy for species VIII was calculated at χ = 60°. This conformation is compatible with the results obtained from analysis of the pmr spectrum of 7-epiclindamycin in D_2O solution.§§ However, the model exhibits another low-energy conformation, when χ = 180°, that may be populated to a significant extent.

The calculations performed with species IX-XII were designed, in part, to study the effects of long-range interactions between portions of the carbohydrate moiety and pyrrolidine ring in models resembling lincomycin and clindamycin. Only a few conformations were selected to check the validity of results yielded by models I, II, V, and VII. In referring to structures IX and X, the values of θ, χ, and ω serve to fix the conformation employed in a particular calculation since bond lengths, bond angles, and all other torsional angles were taken from the X-ray structure. Similarly, the values of θ and χ suffice to describe the conformations of XI and XII. Henceforth, a particular conformation will be designated by notation (θ,χ,ω), where the values of the angles are given in the order shown. In the species containing a 7-Cl substituent in place of 7-OH, the angle ω is deleted from the notation.

The calculated conformational energies obtained for the selected conformations of IX-XII are listed in Table IV. In structures IX and X, values of θ were taken as either 300°, corresponding to the favored conformation of species I, or 97.98°, taken from the X-ray structure of lincomycin hydrochloride. Analogously, θ was chosen to be either 300° or 117.5° in XI and XII. The values of χ and ω in IX and X were taken from the two lower energy conformations of V. In structures XI and XII, the value of χ from the X-ray structure of clindamycin hydrochloride was utilized, since it also produced the best calculated energy in species VII.

In some cases, the long-range interactions embodied in IX-XII cause significant quantitative differences in conformational energies relative to the energies obtained with I, II, V, and VII. For example, the difference between conformations with θ = 97.98° and θ = 300° is approximately 20 kcal/mol in species I and 12 kcal/mol in species IX. Large differences are also noted between the results obtained with species II and X in which N(1′) is protonated. Nevertheless, models IX-XII yield conclusions in qualitative agreement with the results of the simpler models.

Molecular Orbital Structure. Preliminary calculations showed that the highest pair of occupied molecular orbitals as well as the lowest unoccupied molecular orbital of I was localized in the amide unit, even with a methyl group substituted for the hydrogen [H(1′)] at the pyrrolidine nitrogen [N(1′)] and/or a propyl group substituted for a hydrogen [H(4′β)] at the trans 4′ position of the pyrrolidine ring. Therefore, the chemically most interesting molecular orbitals (the higher occupied and lower unoccupied molecular orbitals) could be studied without the presence of the methyl or propyl groups mentioned above, which are found on the pyrrolidine ring of lincomycin. These groups do, however, affect the biological activity of lincomy-

§§The coupling constant J_{67} is approximately 3 Hz while J_{56} is roughly 10 Hz. These values suggest that H(6) is gauche to H(7) and trans to H(5) in D_2O solution of 7-epiclindamycin.

Table II. Conformational Energies as a Function of χ in the Clindamycin Moiety, VII

Conformation	χ, deg	ΔE, kcal/mol
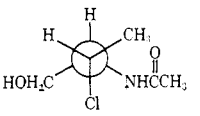	300	0.0
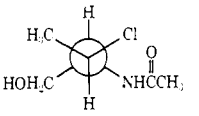	60	12.9
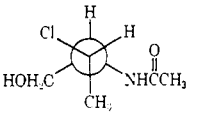	180	18.9

Table III. Conformational Energies as a Function of χ in the 7-Epiclindamycin Moiety, VIII

Conformation	χ, deg	ΔE, kcal/mol
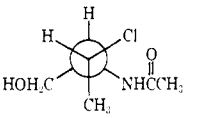	60	0.0
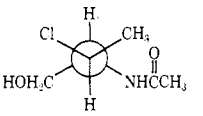	180	1.0
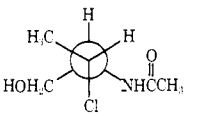	300	4.2

Table IV. Conformational Energies of Lincomycin and Clindamycin Moieties IX-XII

Moiety	Conformation	Conformational energy[a]
IX	(300,180,60)	0.0
	(300,60,300)	1.9
	(97.98,180,60)	12.5
	(97.98,60,300)	13.7
X	(97.98,180,60)	0.0
	(97.98,60,300)	5.0
	(300,180,60)	32.9
	(300,60,300)	40.1
XI	(300,298.8)	0.0
	(117.5,298.8)	16.3
XII	(117.5,298.8)	0.0
	(300,298.8)	52.5

[a]Energy given in kilocalories per mole relative to the conformation of a particular moiety with the lowest calculated energy.

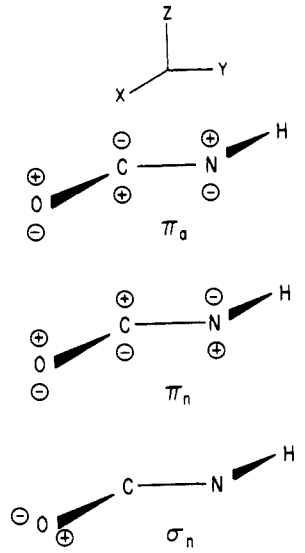

Figure 8. Local amide unit orbital symmetries.

cin,[12,35-38] but the results of the current study indicate that it is unlikely that their role is an electronic one. The propyl group appears to function as a "space filler" for a good fit at the active site and/or increases the lipophilicity of the molecule so as to improve transport across the cell membrane.

As noted earlier, with a few exceptions, the next to highest occupied MO (NHOMO), highest occupied MO (HOMO), and the lowest unoccupied MO (LUMO) in each of I-IV are quite localized in the amide unit and may be identified as having the symmetries of the highest pair of occupied MO's (σ_n,π_n) and lowest unoccupied MO (π_a) of formamide (see Figure 8). Assuming that nucleophilic attack will occur most readily at the sites defined by the LUMO and electrophilic attack will occur most readily at the HOMO, it may be concluded that reactivity will be centered primarily at the amide unit, and modifications of the molecular structure that affect the MO's located in the vicinity of the amide unit may have marked effects on the reactivity of the molecule.

In all species, I-XIII, the LUMO is localized in the amide unit and has π_a symmetry. In species I, II, IV-IX, and XI, the HOMO is localized in the amide unit and has π_n symmetry. In III, the HOMO is primarily of σ_n symmetry in the amide unit, and there are also secondary contributions from the pyrrolidine nitrogen lone-pair region. The HOMO in X is dominated by contributions from the lone-pair orbitals of O(1), O(4), and O(7). In XII, the lone-pair orbitals of O(1) and O(4) are major contributors to the HOMO.

The NHOMO in I, II, and V-VIII is localized in the amide unit and has σ_n symmetry. The NHOMO in III is a π_n MO localized in the amide unit. The NHOMO in IV is localized in the pyrrolidine nitrogen lone-pair region. In IX and X, the NHOMO is dominated by contributions from the lone-pair orbitals of O(1), O(4), and O(7). The lone-pair orbitals of O(1) and O(4) are the primary contributors to the NHOMO of XI and XII. Apparently, hydrogen bonding interactions between 4-OH and O(A) serve to stabilize the amide σ_n orbital in IX and XI relative to V and VII.

It should be noted that protonation of the pyrrolidine nitrogen in I to obtain II causes a marked lowering of the orbital energies of the NHOMO, HOMO, and LUMO. The same effect was observed in comparing IX and XI with their respective protonated counterparts, X and XII. Assuming that changes in orbital energies may be correlated with changes in reactivity, the protonated species would be expected to be more susceptible to nucleophilic attack and less susceptible to electrophilic attack at sites in the amide moiety.

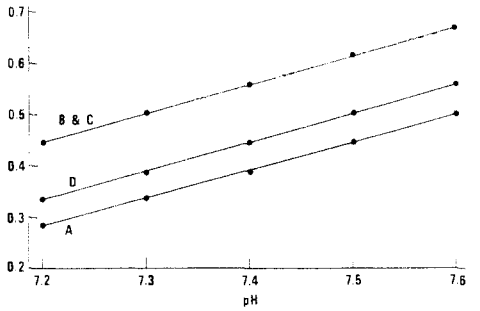

Figure 9. Fraction (f) of drug concentration in unprotonated form as a function of the pH for lincomycin (A), 7-epilincomycin (B), clindamycin (C), and 7-epiclindamycin (D).

Discussion

In examining the data obtained from the quantum mechanical studies just described, it appears that several points, both specific and general, can be made regarding the electronic and geometric structure of lincomycin and its analogs, and their relationship to the activity of the drugs. The data from the current studies are, of course, best utilized in conjunction with *in vitro* results rather than *in vivo* results.

The role of the hydrocarbon side chain attached to the pyrrolidine ring at the 4 position appears to be simply that of a "space filler" for a good fit at the active site and/or as a lipophilic moiety to increase the lipophilicity of the entire molecule, and in doing so, to improve transport across the cell membrame. The hydrocarbon side chain does not significantly perturb the electronic structure of the amide unit.

The conformational energy studies indicate that the unprotonated [at pyrrolidine nitrogen, N(1′)] form of lincomycin, which is believed to be the form responsible for antibacterial activity,[12] is most stable in an approximately planar five-membered ring structure, stabilized by a hydrogen bond between the amide hydrogen and the pyrrolidine nitrogen. The observed *in vitro* activity of the formaldehyde condensation products (similar to V), which are held in the approximate preferred conformation (θ = 300°) of unprotonated lincomycin because of the constraint of ring formation, supports this observation.

The calculations performed with models IX-XII indicate that long-range steric interactions between the carbohydrate and pyrrolidine moieties are significant but do not alter the conclusions derived from simpler models regarding molecular conformation of a given analog. However, when comparing different analogs having modifications at C(7), the relative stabilities of the protonated and unprotonated species could be affected by changing the nature and magnitude of the long-range interactions.

An experimental measure of these effects is provided by the differences in pK_a among the lincomycin analogs with modifications at C(7). As shown in Figure 9, if the pH of the medium is in a range roughly corresponding to that of human blood, a significantly greater proportion of clindamycin molecules (pK_a ≈ 7.3) will exist in the unprotonated form than of 7-epiclindamycin (pK_a ≈ 7.5), as might be expected from the relative activities of these analogs. On the other hand, lincomycin (pK_a ≈ 7.6) will have a smaller unprotonated population than the less active analog, 7-epilincomycin (pK_a ≈ 7.3), under the same pH conditions. If the uncharged molecule is required for opti-

mal passage through the bacterial cell wall, 7-epilincomycin should reach the receptor site in greater concentration than lincomycin. Hence, it would appear that other factors are responsible for the low level of activity of 7-epilincomycin. Quantitative comparison between the 7-Cl and 7-OH analogs must take into consideration the difference in lipid-water solubility of the uncharged species as well as pK_a differences. However, the differences in pK_a between the 7-Cl analogs and lincomycin indicate that the relative concentrations of unprotonated molecules could partially account for the relative *in vitro* activities of these drugs.

In comparing the preferred geometries found for each of the 7-substituted analogs, it is seen that the 7-epilincomycin model, unlike the others, forces a relatively bulky C(7) substituent to occupy the position trans to the amide group. Although the lincomycin and 7-epiclindamycin models also yield low-energy conformations with OH or Cl trans to the amide, alternative conformations with similar energies are found to be available for these analogs in which H(7) is located in that position. On the basis of these findings, the low activity of 7-epilincomycin could result from adverse steric interactions involving 7-OH which reduce the affinity of the drug for the receptor.[==]

The available data can also be used to predict results for similar molecules that were not included explicitly in the calculations, namely, the 7-methoxy analogs. Since the stability of the conformation with $\chi = 180°$ in 7-epilincomycin results from the formation of an intramolecular hydrogen bond between HO(7) and O(1), replacement of HO(7) by a methyl group will alter the conformation about the C(6)–C(7) bond. Thus, for example, the preferred value of ω [$\angle$C(6)–C(7)–O(7)–CH_3] in 7(*S*)-methoxy-7-deoxylincomycin will likely be 180° in order to minimize steric interactions between the methyl group attached to O(7) and the bulky groups attached to C(6). In this case, the points in Figure 7 corresponding to $\omega = 180°$ may be expected to give reasonable estimates of the conformational energies resulting from different values of χ. Comparison of these points shows that the conformation with $\chi = 300°$ is considerably more stable than the other two staggered conformations. Hence, the unprotonated form of this molecule is predicted to assume the conformation (300,300,180) which places OCH_3 in the same spatial location as Cl in clindamycin. It is interesting to note that the 7(*S*)-OCH_3 analog is as active as clindamycin in the standard plate assay with *S. lutea*.[39] Using a similar line of reasoning and the data in Figure 6, unprotonated 7(*R*)-methoxy-7-deoxylincomycin is predicted to have two equally stable conformations, (300,60,180) and (300,180,180). This analog exhibits an *in vitro* activity of 1.3 relative to lincomycin against *S. lutea*.[40] Thus, neither of the 7-methoxy analogs forces a group bulkier than a hydrogen atom to assume a position trans to the amide unit, and both are more active than lincomycin.

Conclusions

The model structures studied in this work serve to demonstrate a number of effects associated with various modifications of the pyrrolidine ring and the sugar side chain in lincomycin. The geometric and electronic changes accompanying protonation of the amine nitrogen, N(1′), may be highly important since the free base appears to be more active than the quaternary salt. Of particular interest is the stabilization of the amide π_a, π_n, and σ_n orbitals caused by protonation. Alterations at C(7) in the carbohydrate moiety lead to variations in long-range steric interactions between the C(7) substituents and moieties of the pyrrolidine ring, which affect the relative stabilities of the protonated and unprotonated species. Stabilization of a sugar side-chain conformation with a bulky group trans to the amide unit appears to have a deleterious effect on the antibacterial activity, possibly due to unfavorable steric interactions at the receptor.

Acknowledgments. The authors would like to express their appreciation to the University of Kansas for partial support of the computing required for this study. In addition, T. E. Eble and B. Bannister of The Upjohn Co. must be thanked for many enlightening discussions during the course of this work.

References

(1) D. F. Mason, A. Dietz, and C. Deboer, *Antimicrob. Ag. Chemother.*, 554 (1962).
(2) R. R. Herr and M. E. Bergy, *Antimicrob. Ag. Chemother.*, 560 (1962).
(3) L. J. Hanka, D. J. Mason, M. R. Burch, and R. W. Treick, *Antimicrob. Ag. Chemother.*, 565 (1962).
(4) C. Lewis, H. W. Clapp, and J. E. Grady, *Antimicrob. Ag. Chemother.*, 570 (1962).
(5) F. N. Chang, C. J. Sih, and B. Weisblum, *Proc. Nat. Acad. Sci. U. S.*, **55**, 431 (1966).
(6) D. Vazquez and R. E. Monro, *Biochim. Biophys. Acta*, **142**, 155 (1967).
(7) R. E. Monro and D. Vazquez, *J. Mol. Biol.*, **28**, 161 (1967).
(8) J. M. Wilhelm, N. L. Oleinick, and J. W. Corcoran, *Antimicrob. Ag. Chemother.*, 236 (1967).
(9) B. Weisblum and J. Davies, *Bacteriol. Rev.*, **32**, 493 (1968).
(10) K. Igarashi, H. Ishituka, and A. Kaji, *Biochem. Biophys. Res. Commun.*, **37**, 499 (1969).
(11) J. B. Meilck and E. R. Garrett, *Chemotherapy*, **14**, 337 (1969).
(12) S. M. Heman-Ackah and E. R. Garrett, *J. Med. Chem.*, **15**, 152 (1972).
(13) R. Fernandez-Muñoz, R. E. Monro, R. Torrez-Pinedo, and D. Vazquez, *Eur. J. Biochem.*, **23**, 185 (1971).
(14) B. V. Cheney, *J. Med. Chem.*, **17**, 590 (1974).
(15) B. J. Magerlein, *Advan. Appl. Microbiol.*, **14**, 185 (1971).
(16) R. E. Christoffersen and G. M. Maggiora, *Chem. Phys. Lett.*, **3**, 419 (1969).
(17) R. E. Christoffersen, D. W. Genson, and G. M. Maggiora, *J. Chem. Phys.*, **54**, 239 (1971).
(18) G. M. Maggiora, D. W. Genson, R. E. Christoffersen, and B. V. Cheney, *Theor. Chim. Acta*, **22**, 337 (1971).
(19) R. E. Christoffersen, L. L. Shipman, and G. M. Maggiora, *Int. J. Quantum Chem.*, **5S**, 143 (1971).
(20) R. E. Christoffersen, *J. Amer. Chem. Soc.*, **93**, 4104 (1971).
(21) R. E. Christoffersen, *Advan. Quantum Chem.*, **6**, 333 (1972).
(22) B. V. Cheney and R. E. Christoffersen, *J. Chem. Phys.*, **56**, 3503 (1972).
(23) D. W. Genson and R. E. Christoffersen, *J. Amer. Chem. Soc.*, **94**, 6904 (1972).
(24) L. L. Shipman and R. E. Christoffersen, *Chem. Phys. Lett.*, **15**, 469 (1972).
(25) L. L. Shipman and R. E. Christoffersen, *Proc. Nat. Acad. Sci. U. S.*, **69**, 3301 (1972).
(26) D. W. Genson and R. E. Christoffersen, *J. Amer. Chem. Soc.*, **95**, 362 (1973).
(27) L. J. Weimann and R. E. Christoffersen, *J. Amer. Chem. Soc.*, **95**, 2074 (1973).
(28) L. L. Shipman and R. E. Christoffersen, *J. Amer. Chem. Soc.*, **95**, 4733 (1973).
(29) R. E. Christoffersen, *Int. J. Quantum Chem.*, in press.
(30) L. L. Shipman and R. E. Christoffersen, *Theor. Chim. Acta*, **31**, 75 (1973).
(31) R. E. Davis and R. Parthasarathy, *Acta Crystallogr., Sect. A*, **21**, 109 (1966).
(32) J. W. Turley and R. Pepinksy, *Acta Crystallogr.*, **10**, 480 (1957).
(33) G. Slomp and F. A. MacKellar, *J. Amer. Chem. Soc.*, **89**, 2454 (1967).

[==]According to the theoretical model for the antibacterial activity of lincomycin outlined in ref 14, O(1) is involved in binding at the ribosome. Since the intramolecular hydrogen bond between HO(7) and O(1) in 7-epiclindamycin would effectively preclude interaction with the ribosome at O(1), the low activity might also result from this circumstance.

(34) R. E. Christoffersen, D. Spangler, G. G. Hall, and G. M. Maggirora, *J. Amer. Chem. Soc.*, **95**, 8526 (1973).
(35) B. J. Magerlein, R. D. Birkenmeyer, and F. Kagan, *Antimicrob. Ag. Chemother.*, 727 (1966).
(36) B. J. Magerlein, R. D. Birkenmeyer, and F. Kagan, *J. Med. Chem.*, **10**, 355 (1967).
(37) B. J. Magerlein and F. Kagan, *J. Med. Chem.*, **12**, 780 (1969).
(38) Y. C. Martin and K. R. Lynn, *J. Med. Chem.*, **14**, 1162 (1971).
(39) B. Bannister, *J. Chem. Soc., Perkin Trans. 1*, in press.
(40) B. Bannister, *J. Chem. Soc., Perkin Trans. 1*, 1676 (1973).

Ab Initio Calculations on Large Molecules Using Molecular Fragments. Structural Correlations between Natural Substrate Moieties and Some Antibiotic Inhibitors of Peptidyl Transferase

B. Vernon Cheney

Research Laboratories of The Upjohn Company, Kalamazoo, Michigan 49001. *Received October 29, 1973*

Lincomycin, chloramphenicol, and erythromycin are antibiotic inhibitors of bacterial protein synthesis which are postulated to act by blocking the peptidyl transferase site at the 50S ribosomal subunit. Correlations between structural features of these antibiotics and the terminal moieties of the natural substrate molecules, peptidyl and aminoacyl tRNA, aid in rationalizing the observed competitive binding of these species at the catalytic site for peptide bond formation. Investigations of the electronic and geometric structure of the terminal moiety of peptidyl tRNA have been carried out using the *ab initio* SCF-FSGO method with 3-*O*-(*N*-glycylglycyl)ribose as a model. These studies give insight into the relationship between chemical structure and biological activity for the natural substrate as well as the antibiotic inhibitors of peptidyl transferase. The results of the studies indicate that it is not necessary to postulate allosteric mechansims of action to explain the effects of the drugs.

Lincomycin, chloramphenicol, and erythromycin are antibiotics with diverse molecular structures which, nevertheless, produce similar effects in various experiments designed to study their mode of action. All three antibiotics inhibit ribosomal protein synthesis while allowing RNA and DNA synthesis to continue.[1-3] Each of the drugs forms a reversible one-to-one complex with the 50S subunit of the bacterial ribosome.[4-7] Furthermore, competition for binding at the ribosome occurs when any two of the three antibiotics are present in the system.[7,8] In studies[9-13] using the puromycin reaction to model ribosome-catalyzed peptide bond formation, the drugs produce marked inhibitory effects, although the extent of inhibition depends on the assay employed. These facts led Monro, *et al.*,[14] to suggest that the antibiotics bind at overlapping sites at the peptidyl transferase center of the 50S ribosomal subunit.

Interesting differences in the actions of lincomycin, chloramphenicol, and erythromycin have been noted by various workers. Certain erythromycin-resistant strains of *Staphylococcus aureus* display cross resistance toward lincomycin but not chloramphenicol.[15,16] The three antibiotics also exhibit different effects on substrate binding at the peptidyl transferase center of the 50S subunit.[17-20] For example, erythromycin appears to stimulate binding of CACCA-Leu and CACCA-(Ac-Leu) while lincomycin inhibits the binding of both fragments. On the other hand, chloramphenicol apparently stimulates binding of the Ac-Leu substrate and inhibits the binding of the Leu substrate. As stated by Monro, *et al.*,[14] different effects, such as these, could be observed even if the antibiotics bind at overlapping sites since the molecules differ in size, shape, and other properties. However, some investigators[21,22] have suggested that the drugs must act through allosteric mechanisms on account of these dissimilar effects.

In the current study, various structural relationships are noted between lincomycin, chloramphenicol, erythromycin, and a moiety of peptidyl tRNA which is postulated to bind at the locus of peptidyl transferase. The structural correlations are employed to develop a simple chemical model for the mechanism of peptide bond formation at the ribosome and the interactions of the drugs at the peptidyl transferase center. Many similarities and differences in the effects of the three antibiotics may be rationalized in terms of the model. In addition, the model provides a basis for understanding relationships between biological activity and features of the chemical structure exhibited by several drug analogs.

Description of Model. The process of bacterial protein synthesis requires binding of peptidyl tRNA at the P site and aminoacyl tRNA at the A site of the 70S ribosome.[23,24] Since template mRNA is bound at the 30S subunit, the interaction with tRNA in that portion of the ribosome involves codon-anticodon recognition which determines the sequence of amino acids in the protein. Specific binding to the 50S ribosomal subunit occurs in the region of the peptidyl transferase catalytic center. Monro, *et al.*,[14] have proposed that interactions at the P site of peptidyl transferase involve the 3′-terminal nucleotide grouping CCA, which is common to all species of tRNA, and are favored by acylation of the α-NH_2 group of the attached amino acid. They also suggested that the terminal CA binds specifically at the A site of peptidyl transferase.

The reaction to form the peptide bond may be postulated to occur as shown in Scheme I where T_nOH is the carrier tRNA molecule for the amino acid with side chain R_n and X denotes the previously synthesized segment of the protein chain. Although the species designated as III may only have a transitory existence, the primary function of peptidyl transferase would be to facilitate its formation and direct its break-up into the elongated peptidyl tRNA molecule, IV, and the released tRNA molecule, V. Thus, it would be possible to make useful inferences regarding the nature and relative positions of ribosomal binding sites at the peptidyl transferase center if the detailed structural features of III were known. By considering a system consisting only of the terminal adenosine nucleotide of tRNA and the attached peptidyl or aminoacyl groups, a simple model for species III is developed in succeeding paragraphs.

If lincomycin, chloramphenicol, and erythromycin are specific inhibitors of peptidyl transferase, as indicated by